Electromagnetic steel products: a systematic iron loss evaluating scheme.

Cheng-Tsung Liu, Li-Yang Liu & Shen-Yang Lin.

To sell electromagnetic steel in competitive markets, test results that can properly indicate the iron losses of those products at different specifications are desired. However, the available data sheets can only cover typical data from common Epstein frame tests, and further information regarding possible iron losses beyond the measurement setups can only be estimated by approximations leading to inaccuracies. Based on the Preisach model and available measurements, a systematic scheme to establish a generalized guidance for evaluating the hysteresis characteristics of electromagnetic steel is proposed. Supported by experimental measurements and detailed 3D field analyses, iron losses of those mechanisms constructed by laminated electromagnetic steel can then be estimated with enough confidence.

The Epstein frame test setup

Generally, the measurements are obtained from standard Epstein frame tests. To perform the common Epstein frame test, as shown in Fig. 1, adequate primary winding magnetization current is applied to the testing assembly. The iron core is composed of eight (generally, a multiple of four) identical isotropic/anisotropic electromagnetic steel strips, and the power consumptions associated with specific voltage and current settings can be determined. The current and voltage information can be transformed to the equivalent magnetization field intensity and flux density values. With the secondary windings being open circuited, the measured power consumptions can be viewed as the iron losses of the steel strips.

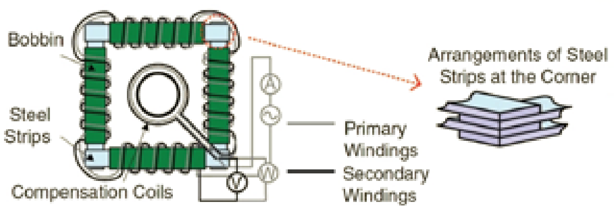

Fig. 1: An illustration of the Epstein frame test.

The data sheets from the manufacturers can thus provide the discrete information of the electromagnetic steel, as shown in Fig. 2.

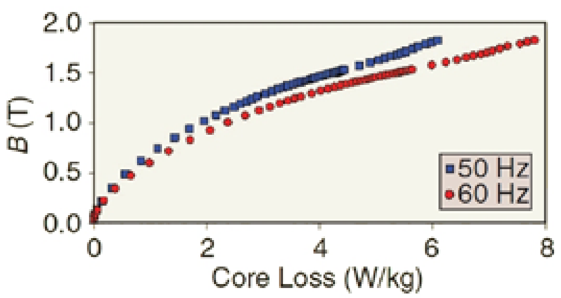

Fig. 2: Iron losses of a magnetic steel obtained from Epstein frame test.

However, since the attainable measurements are limited, the available data sheets can only cover typical information, and estimated additional data regarding possible iron losses beyond the conducted measurement setups can introduce inaccuracies due to generally non-uniformly distributed flux densities.

Without the detailed flux distribution patterns and their corresponding density levels at those specific mechanisms, it is impossible to supply data sheets that can fit exactly to the customers' requirements. Therefore, based on the modelled steel, the constructed Epstein frame test system can be emulated by the equivalent circuit shown in Fig. 3. r1, r2, r3 and r4 are, respectively, the resistance values of primary, secondary, and two compensation coil windings ; Ll1, Ll3 and Ll4 are the corresponding leakage inductance at these windings with Ll2 = 0 and Rc is the equivalent resistance to represent eddy-current loss.

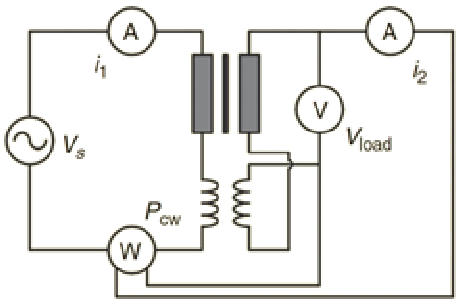

Fig. 3: An equivalent circuit model of the Epstein frame test: (a) physical configuration and (b) emulated equivalent model.

Among that the Preisach model will be adapted to the equivalent mutual inductance (Lm1) to model those flux variations flowing through the steel strips. Since the compensation coils are air-cored, the nonlinear characteristics will not exhibit on their equivalent mutual inductance (Lm3). By using this emulated circuit model, continuous voltages at different levels and frequencies can be applied, and the resultant iron losses can then be calculated from the simulated system voltage and current information. Since the fluxes are generally not uniformly distributed inside the electromagnetic mechanisms, a time-period analytical classification scheme can be used for representing the iron losses with space distributed flux patterns.

The iron loss evaluation procedure

Based on the emulated numerical Epstein frame test system and the Preisach model, current flowing through the equivalent mutual inductance Lm1 with different voltage source input patterns can be adequately modelled. Since the magnetic field intensity flowing through the magnetic steel is linearly proportional to the magnetizing current, the magnetic flux density can be derived from Vm1 by using the relation

(1) $$Bm1 = \frac{\int Vm1.dt}{N1.A}$$

where $Bm1$ is the flux density passing through the magnetic steel core and A is the averaged cross-sectional area of the magnetic flux path in the Epstein frame test with

(2) $$A = \frac{m}{4.L.\rho m}$$

in which m is the total weight of the magnetic steel specimens, L is the length of individual specimen and ρm is the density of the specimen.

By using the standard measurement data as provided by the magnetic steel manufacturer and the proposed numerical Epstein frame test model, the iron loss, which can be divided into two parts, namely the hysteresis and the eddy-current losses, can now be systematically estimated from the aforementioned formulations and experiments.

From those standard Epstein frame tests performed by the manufacturers, averaged equivalent resistance Rc for the entire operational voltage range can be calculated. Since this loss component is basically not closely related to the magnetizing current, those nonlinear characteristics

(continued on page 7)

resulting from the magnetic saturation and hysteresis can be ignored. Therefore, from the circuit definition, we can express the eddy-current loss Pe as

$$Pe = \frac{Vm1^2}{Rc} \quad (3)$$

The desired hysteresis losses for different electromechanical mechanisms constructed by electromagnetic steel at various applied magnetizing inputs can be systematically estimated. Using uniformly distributed magnetic flux on the devised model to properly predict the iron losses, the analyzed mechanism must be first divided into several modules. Then the calculated hysteresis losses at these modules will be assembled together to provide total system hysteresis losses.

Confirmation of the modularized iron loss evaluation procedure

To confirm the adequacy of the emulated Epstein frame circuit model, a 300 W, three-phase, 60 Hz, 190.5 V synchronous switched-reluctance motor (SRM) with six stator poles and four rotor poles has been selected for assessment comparisons. Both the stator and the rotor iron cores are assembled by CSC 50CS470.
Based on the iron loss information as provided by the manufacturer, the total iron loss can be roughly estimated at the level of 19.18 W in so far as the iron loss per unit weight of CSC 50CS470 is 3.461 W/kg and the total weight of the magnetic steel for constructing the motor is 5.54 kg. Since the magnetic fluxes inside the motor will not be uniformly distributed in practical cases, detailed calculations of the magnetic fields based on FEA (Flux2D/3D software) are introduced to supply comprehensive system information. Along with proper data postprocessing, the total iron loss of the test motor at rated operational condition can then be calculated.

By comparing this with those obtained from the rough estimation, the result showed that a much different level of 5.51 W will be derived.
The total motor iron loss estimations as obtained from the above two schemes will exhibit a relative difference of above 248 %. Although the ones calculated from 3D FEA along with some postprocessing works are based on empirical Steinmetz's relationship, these are much more reliable than those rough estimations since the flux density distributions of the motor at a complete rotation cycle have been carefully taken into account. Thus, motor manufacturers will generally rely on the FEA calculated results rather than the rough estimation from the magnetic steel data sheets.

The proposed scheme

It is apparent from Fig. 4 that the non-uniformly distributed flux density patterns will rotate on the motor operational direction, which means that the maximum flux density (1.32 T) will pass through specific motor regions periodically, and not all the regions.

Therefore, by dividing the motor cross-sectional surface into several regions and assuming that the flux densities at all positions inside every individual region are identical, the equivalent iron losses at these regions can then be calculated systematically based on the emulated Epstein frame test results and their specific operational frequencies.
As illustrated in Fig. 5 (a), one of the six stator poles is selected and divided into eight regions. The magnetic fluxes distributed on the selected pole at the same time instance (Fig. 4) are expanded in Fig. 5 (b) to provide a clearer description. By checking the magnetic flux densities, it can be seen that the assumption of identical flux densities can be reasonably achieved if larger number regions can be divided. Nevertheless, by averaging the 2D flux densities inside this region, their corresponding flux linkages can be evaluated and the induced voltage can be obtained from (1).

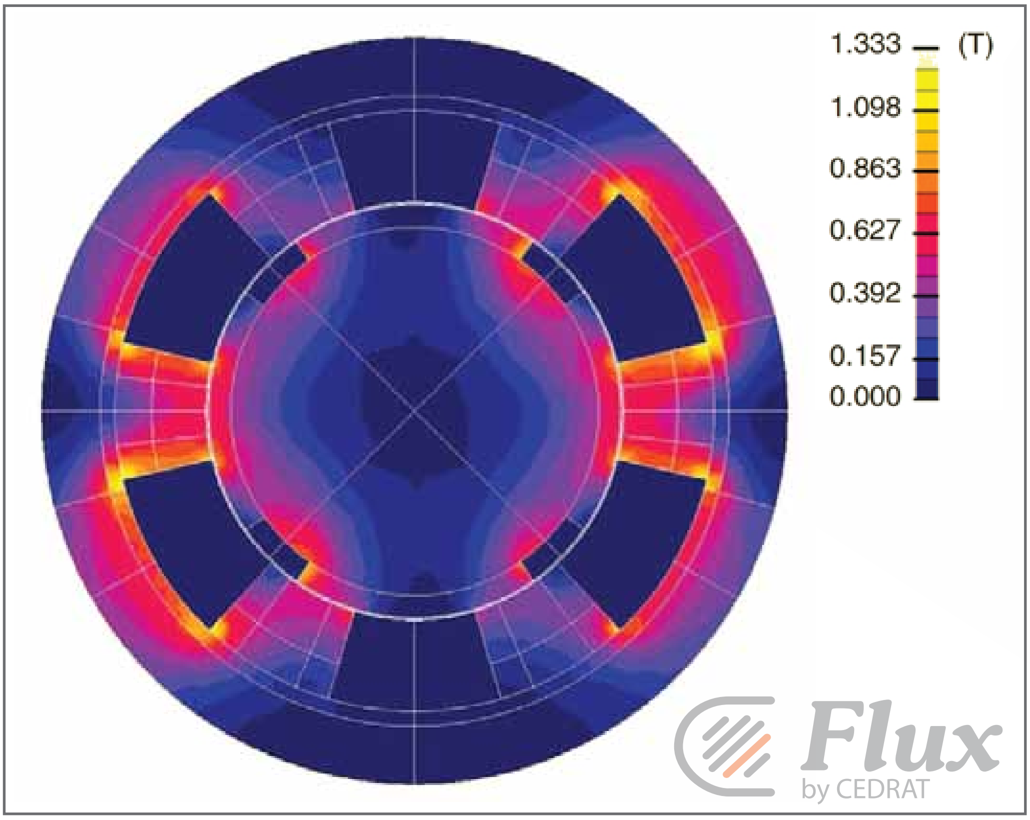

Fig. 4: Through flux density distribution of the test motor at one time instance obtained from 2D FEA.

(continued on page 8)

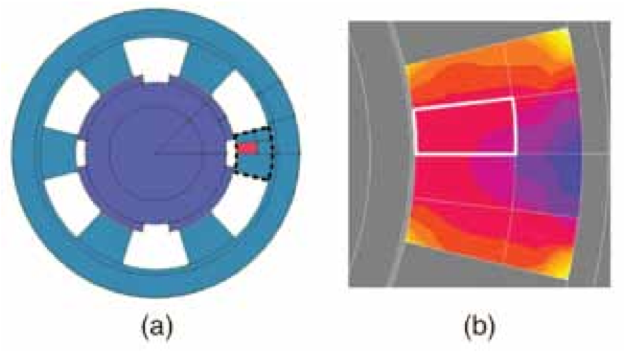

Fig. 5: Selected regions for estimating the motor iron loss: (a) stator pole and region partitions and (b) magnetic flux distribution at the stator pole.

The desired voltage input patterns can then be calculated by following the equivalent circuit model as shown in Fig. 3 and the basic magnetization curve as

(4a) $$i_{li} = i_{mli} + \frac{V_{mli}}{R_c}, i = x, y$$ and

(4b) $$V_{si} = (r_1 + r_3).i_{li} + \frac{d}{dt}[(L_{l1} + L_{l3} + L_{m3}).i_{li}] + V_{mli}$$

The devised individual voltage pattern is then applied to the proposed equivalent circuit model that can emulate the Epstein frame state to calculate the desired system operational information. Fig. 6 shows the time-dependent 2D flux densities and their corresponding calculated input voltage patterns Vsx and Vsy for performing the required Epstein frame test emulations in the selected region.
It can be observed that higher order harmonics are exhibited in these

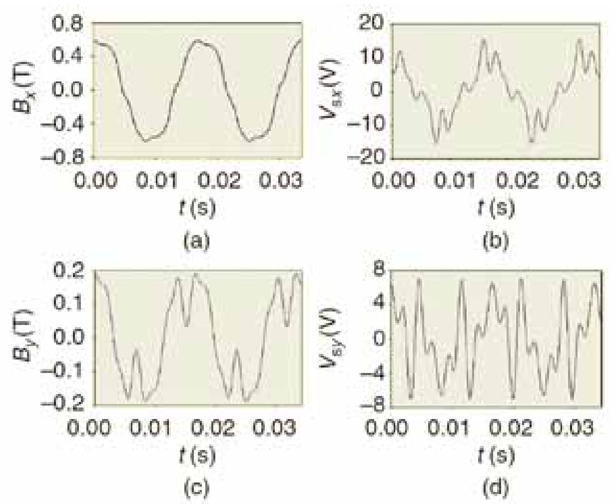

Fig. 6: 2D flux densities and calculated voltage input patterns: (a) x-directional flux density, (b) calculated voltage input pattern Vsx, (c) y-directional flux density, (d) calculated voltage input pattern Vsy.

voltage patterns due to machine structure, and the hysteresis inner-loop effects will inevitably contribute to the iron loss calculations. Based on the obtained circuit variables and the expressions as indicated in (4), iron loss of the selected region with unit depth can be calculated.
Therefore, total iron loss of the test motor can then be systematically derived by accumulating the individual ones of all the regions together. With every half of the stator pole and rotor pole being partitioned into the regions as that shown in Fig. 5 (a), the entire machine can be divided into 128 regions.

Such scheme will provide a total iron loss of 5.68 W which is only about 3.07 % different from that obtained from detailed FEA. Adequacy and accuracy of the proposed iron loss derivation scheme can then be confirmed.

Validations

Comparisons of the iron loss evaluations of a 6/4 synchronous SRM by different schemes have been performed. Although it can be demonstrated that the proposed scheme will supply the results with better accuracy, the number of regions that were divided in the entire machine analyses will greatly affect the confidences of the iron loss estimations. The summarized comparisons are provided in Table 1.

Table 1. Iron loss information of the test 6/4 synchronous SRM estimated by different schemes					
	Proposed Scheme				
Item	3D FEA	Rough Estimation	128 Regions	84 Regions	32 Regions
Iron loss (W)	5.51	19.18	5.68	4.84	4.12
Difference (%)	--	248.09	3.09	-12.16	-25.23

Table 1. Iron loss information of the test 6/4 synchronous SRM estimated by different schemes.

By using the same CSC 50CS470 steel, the iron losses of two other 6/4 synchronous SRMs at different sizes have been evaluated and the results are provided in Table 2 for comparison.

Table 2. Iron Loss information of three 6/4 synchronous SRMs estimated by the proposed schemes			
Item	Motor A	Motor B	Motor C
Power rating (W)	300	130	100
Iron loss by 3D FEA (W)	5.51	1.43	0.94
Maximum air-gap flux density (T)	0.51	0.44	0.34
Iron loss by the proposed scheme (W)	5.68	1.82	1.08
Difference (%)	3.09	27.27	14.89

Table 2. Iron Loss information of three 6/4 synchronous SRMs estimated by the proposed schemes.

The number of regions in the machine analyses has been fixed at 128. Although the results shown on the last two columns for motors B and C are not that attractive at those obtained from motor A, the derivation efficiency and compactness still demonstrated that a much reliable iron loss estimation scheme can be provided.

Conclusion

Instead of using the detailed and time-consuming 2D or 3D FEA, the commonly used estimations generally provide information that are far from the exact ones. By combining the measured magnetization characteristics from the steel manufacturers and the theoretical Preisach models, this article has proposed a numerical scheme that can emulate the Epstein frame test to calculate the associated iron losses with different magnetization input voltage patterns.

Flux by CEDRAT